J. Fluid Mech. (1988), *vol.* 186, *pp.* 445–469
Printed in Great Britain

On the secondary instability of Taylor–Görtler vortices to Tollmien–Schlichting waves in fully developed flows

By JAMES BENNETT AND PHILIP HALL
Mathematics Department, Exeter University, Exeter EX4 4QE, UK

(Received 8 December 1986 and in revised form 6 July 1987)

There are many flows of practical importance where both Tollmien–Schlichting waves and Taylor–Görtler vortices are possible causes of transition to turbulence. In this paper, the effect of fully nonlinear Taylor–Görtler vortices on the growth of small-amplitude Tollmien–Schlichting waves is investigated. The basic state considered is the fully developed flow between concentric cylinders driven by an azimuthal pressure gradient. It is hoped that an investigation of this problem will shed light on the more complicated external-boundary-layer problem where again both modes of instability exist in the presence of concave curvature. The type of Tollmien–Schlichting waves considered have the asymptotic structure of lower-branch modes of plane Poiseuille flow. Whilst instabilities at lower Reynolds number are possible, the former modes are simpler to analyse and more relevant to the boundary-layer problem. The effect of fully nonlinear Taylor–Görtler vortices on both two-dimensional and three-dimensional waves is determined. It is shown that, whilst the maximum growth as a function of frequency is not greatly affected, there is a large destabilizing effect over a large range of frequencies.

1. Introduction

In laminar boundary-layer flows over a surface, such as a wing, shear-flow instabilities in the form of Tollmien–Schlichting waves can occur. These waves are the subject of much theoretical and experimental interest since it is thought that they cause transition to turbulence. When the flow is over a curved surface, centrifugal instabilities such as Taylor or Görtler vortices may also be present. These may interfere destructively with the Tollmien–Schlichting waves and thereby delay transition. Alternatively, by making the flow three-dimensional, they could play an essential part in the process of transition. The interaction of these two types of instabilities is therefore of some theoretical importance and has practical applications in the development of laminar-flow wings.

Hall & Bennett (1986) showed that when Tollmien–Schlichting waves travel past a curved boundary, an unstable Stokes layer forms on the wall, and it was suggested there that the growth of longitudinal vortices in this Stokes layer could destroy the Tollmien–Schlichting waves. In this paper, we consider the opposite problem, namely the stability of a Dean (1928) type Taylor vortex in a channel to small-amplitude travelling waves. By comparing our results with the stability analysis of a channel flow without any vortex motion, we hope to be able to tell whether the presence of the vortices hinders or enhances the growth of the Tollmien–Schlichting waves. A related problem was studied by Nayfeh (1981) in which Görtler vortices

were allowed to interact with oblique Tollmien–Schlichting waves. There the Görtler vortex was determined by solving the parallel-flow linear instability equations and had its amplitude assigned arbitrarily. Such a procedure could lead to incorrect results because Hall (1982*a*, 1983) has shown that non-parallel effects cannot be ignored in the linear Görtler instability problem. Moreover, a finite-amplitude Görtler vortex has its amplitude determined by the Görtler number and cannot be specified arbitrarily. Furthermore, in the only case where a non-parallel theory of nonlinear Görtler vortices has been given (Hall 1982*b*), the mean flow distortion induced by the fundamental is the same size as the fundamental. In such a situation, it is clear that the contribution of the mean flow correction and its harmonics cannot be ignored. The channel flow considered here does not vary in the streamwise direction, so non-parallel effects do not occur. Bennett (1986), however, has shown that our analysis does apply to external non-parallel flows, though results for that problem will not be available until the fully nonlinear Görtler problem in external flows has been solved numerically.

We confine our attention to the linear stability of the vortex motion at high Reynolds numbers. Furthermore, we shall concentrate on the lower branch of the neutral curve, so that the Tollmien–Schlichting waves are governed by interactive boundary-layer theory. This case describes asymptotically almost all the unstable range of high-Reynolds-number disturbances. In §2 we derive the dispersion relation linking the wave frequency to the wavenumber for waves travelling parallel to the main direction of the flow. This is done in a similar manner to Smith (1979*a*), where the stability of unidirectional flow was considered. The difference between that and the present work is that there the basic flow varied on a cross-stream (z) distance comparable with the long wavelength of the disturbances, whereas the z-variation in our basic flow is governed by the shape of the Taylor vortex. In §§2–6 we consider 'square' Taylor vortices, where the z-variation is comparable with the channel width and therefore much faster than the streamwise (x) variation of the waves. In §§3 and 4 we look at two limits of the dispersion relation derived in §2. First, in §3, we look at what happens when the amplitude of the Taylor vortex is small, so that the vortex is governed by the weakly nonlinear theory of Seminara (1976). Secondly, in §4, we find how the scaled wavenumber α of the Tollmien–Schlichting waves behaves when the scaled wave frequency Ω is large. In §5 we describe the numerical calculations needed to work out the vortex velocity field and to find solutions of the dispersion relation. Section 6 extends these results to the case of waves travelling obliquely to the flow. Finally, in §7, we give a discussion of our results and their relevance.

2. The dispersion relation for small-amplitude Tollmien–Schlichting waves in the presence of fully nonlinear Taylor–Görtler vortices

We take as our basic flow the Taylor vortex that arises in the Dean (1928) problem when incompressible fluid is driven between concentric cylinders by a constant azimuthal pressure gradient. If the radii of the cylinders are a and $a+d$, then we assume that the channel is narrow, that is $\delta = d/a \ll 1$, so that the Taylor vortex is an instability of plane Poiseuille flow, driven by centrifugal forces. If (r^*, θ^*, z^*) are cylindrical polar coordinates, with $r^* = 0$ corresponding to the axes of the cylinders, we define dimensionless coordinates (x, y, z, t) by

$$x = \frac{a\theta^*}{d}, \quad y = \frac{r^*-a}{d}, \quad z = \frac{z^*}{d}, \quad t = \frac{U_m t^*}{dRe},$$

where the Reynolds number $Re = U_m d/\nu$, ν is the viscosity, U_m is a typical mean flow speed and t is a dimensionless time. The dimensionless velocity and pressure of the Taylor vortex, (u, v, w) and p, are given by

$$\boldsymbol{u}^* = U_m\left(U_0+u, \frac{1}{2Re}v, \frac{1}{2Re}w\right), \quad p^* = \rho U_m^2\left(-\frac{12x}{Re}+\frac{p}{Re^2}\right), \tag{2.1}$$

and

$$U_0 = 6y(1-y) \tag{2.2}$$

is the mean flow driven by the pressure gradient.

Substituting these expressions into the Navier–Stokes equations and ignoring terms of $O(\delta)$ and $O(Re\,\delta^2)$, we get

$$\left.\begin{aligned} \frac{\partial v}{\partial y}+\frac{\partial w}{\partial z} = 0, \quad \left(\nabla^2-\frac{\partial}{\partial t}\right)u-\tfrac{1}{2}vU_0' = \mathrm{N}u, \\ \left(\nabla^2-\frac{\partial}{\partial t}\right)\nabla^2 v+TU_0\frac{\partial^2 u}{\partial z^2} = \frac{\partial^2}{\partial z^2}\mathrm{N}v-\frac{\partial^2}{\partial y\,\partial z}\mathrm{N}w-\tfrac{1}{2}T\frac{\partial^2 u^2}{\partial z^2}, \end{aligned}\right\} \tag{2.3}$$

where

$$\nabla^2 \equiv \frac{\partial^2}{\partial y^2}+\frac{\partial^2}{\partial z^2}, \quad \mathrm{N} \equiv \frac{1}{2}\left(v\frac{\partial}{\partial y}+w\frac{\partial}{\partial z}\right). \tag{2.4}$$

The boundary conditions are

$$\left.\begin{aligned} u = v = w = 0 \quad \text{on } y = 0, 1, \\ \text{and} \qquad u, v, w \text{ periodic in } z, \end{aligned}\right\} \tag{2.5}$$

while the Taylor number T has been defined by

$$T = 4Re^2\,\delta. \tag{2.6}$$

The linear instability problem discussed by Dean (1928) can be obtained by linearizing (2.3), so that the right-hand sides vanish, and by replacing $\partial/\partial t$ by σ. If the Taylor number T is plotted against the wavenumber k for steady solutions of Dean's problem, periodic in z with period $2\pi/k$, an open neutral curve typical of convective or centrifugal instabilities is found. Points in (k, T)-space above this neutral curve correspond to unstable linear Taylor vortices, whilst those below represent Taylor vortices that decay to zero when $t \to \infty$. The critical point of the curve is given by $T = T_c = 5161.86$, $k = k_c = 3.951$. Here we are interested in fully nonlinear steady solutions of (2.2)–(2.6). These exist in a region above the linear neutral curve and are obtained numerically in the manner described in §5.

We now consider what happens when the Taylor-vortex velocity (2.1) is perturbed by high-Reynolds-number Tollmien–Schlichting waves travelling parallel to the x-axis. For $Re \gg 1$, the components of velocity in (2.1) perpendicular to the x-axis become negligible. Smith (1979*a*) analysed the stability of a unidirectional flow depending on two spatial variables y and z near the lower branch of the neutral curve when the perturbations vary on a slow x-lengthscale of $O(Re^{\frac{1}{7}})$. In his work, the variation of the basic flow in the cross-stream direction z was also on a long lengthscale of $O(Re^{\frac{1}{7}})$. In this paper, the basic flow varies on a relatively fast $O(1)$ lengthscale in z, forced by the behaviour of the Taylor vortex. There are, however, circumstances in which the z-variation of the Taylor vortex is of $O(Re^{\frac{1}{7}})$, but these occur at much higher Taylor numbers and therefore are not discussed here.

Following Smith, then, but taking into account the different z-scales, we write

$$\epsilon = Re^{-\frac{1}{7}}, \quad x = \epsilon^{-1}X, \quad \hat{T} = \frac{\epsilon^3 U_m t^*}{d}. \tag{2.7}$$

The flow splits up into three regions, an inviscid core, and a viscous critical layer of thickness $O(\epsilon^2)$ on each wall.

In the core, we perturb the Dean problem as follows:

$$\left.\begin{aligned} \boldsymbol{u}^* &= U_m[(\bar{U}, o, o) + (\epsilon^2\hat{u}, \epsilon^3\hat{v}, \epsilon^3\hat{w})E + \ldots], \\ p^* &= \rho U_m^2(\epsilon^4\hat{p}E + \ldots), \end{aligned}\right\} \tag{2.8}$$

where $\bar{U}(y,z) = U_0 + u$ is the velocity of the mean flow and Taylor vortex,

$$E = h\exp(\mathrm{i}(\alpha X - \Omega\hat{T})), \quad h \ll 1, \tag{2.9}$$

and the variables denoted by $\hat{}$ are functions of y and z only. On substituting into the Navier–Stokes equations, we get

$$\mathrm{i}\alpha\hat{u} + \hat{v}_y + \hat{w}_z = 0, \quad \mathrm{i}\alpha\bar{U}\hat{u} + \hat{v}\bar{U}_y + \hat{w}\bar{U}_z = 0, \tag{2.10a,b}$$

$$\mathrm{i}\alpha\bar{U}\hat{v} = -\hat{p}_y, \quad \mathrm{i}\alpha\bar{U}\hat{w} = -\hat{p}_z, \tag{2.10c,d}$$

with slipping conditions at the walls

$$\hat{v} = 0 \quad \text{at } y = 0, 1, \tag{2.11}$$

and $\hat{u}$, $\hat{v}$, $\hat{w}$ and $\hat{p}$ are periodic in z. The scalings for $\hat{u}$, $\hat{v}$ and $\hat{p}$ are those of Smith whilst that for $\hat{w}$ is forced by a comparison of the last two momentum equations (2.10c,d). The velocities in (2.10) can now be written in terms of the pressure

$$\left.\begin{aligned} \nabla^2\hat{p} - \hat{p}_y\frac{\bar{U}_y}{\bar{U}} - \hat{p}_z\frac{\bar{U}_z}{\bar{U}} & \\ (\mathrm{i}\alpha)^2\bar{U}\hat{u} = \nabla^2\hat{p} - \hat{p}_y\frac{\bar{U}_y}{\bar{U}} - \hat{p}_z\frac{\bar{U}_z}{\bar{U}}, & \\ \mathrm{i}\alpha\hat{v} = -\frac{\hat{p}_y}{\bar{U}}, & \\ \mathrm{i}\alpha\hat{w} = -\frac{\hat{p}_z}{\bar{U}}. & \end{aligned}\right\} \tag{2.12}$$

Substituting these expressions into the first momentum equation (2.10b), we get

$$\nabla^2\hat{p} - 2\frac{\hat{p}_y\bar{U}_y}{\bar{U}} - 2\frac{\hat{p}_z\bar{U}_z}{\bar{U}} = 0, \tag{2.13}$$

where ∇^2 is the two-dimensional Laplacian operator defined in (2.4). The boundary conditions (2.11) together with the fact that $\bar{U}$ vanishes at both walls imply that

$$\hat{p}_y = \hat{p}_{yy} = \hat{p}_z = 0 \quad \text{at } y = 0, 1. \tag{2.14}$$

It can be shown from (2.13) and (2.14) that the core problem does not specify $\hat{p}$ uniquely, since for any solution of (2.13) and (2.14) we can add on and multiply by arbitrary constants to get another solution. Thus $\hat{p}$ is determined by the interaction between the core and the viscous layers at $y = 0, 1$.

If $\hat{p} = \phi$ is a solution of (2.13) and satisfies the boundary conditions

$$\phi = 0 \quad \text{at } y = 0, \quad \phi = 1 \quad \text{at } y = 1, \tag{2.15}$$

then it can be shown by series expansions in y and $(1-y)$ that $\hat{p} = \phi$ also satisfies the boundary conditions (2.14). Hence

$$\hat{p} = \hat{p}_0 + (\hat{p}_1 - \hat{p}_0)\phi$$

is also a solution of (2.13) and (2.14) for arbitrary constants $\hat{p}_0$ and $\hat{p}_1$ and is therefore the general solution.

As we move into the lower boundary layer, the core pressure and unperturbed velocity are such that

$$\hat{p} \to \hat{p}_0 + O(y^3), \quad \bar{U} \to \lambda_0(z)\, y \quad \text{as } y \to 0. \tag{2.16}$$

Hence from (2.12) the disturbance velocities are such that

$$\hat{u} \to A_0(z), \quad \hat{v} \to -\mathrm{i}\alpha A_0 y, \quad \hat{w} \sim O(y^2) \quad \text{as } y \to 0. \tag{2.17}$$

The displacement term A_0 satisfies

$$(\mathrm{i}\alpha)^2 \lambda_0 A_0 = \tfrac{1}{2}(\hat{p}_1 - \hat{p}_0)\, \phi_{yyy}|_{y=0}. \tag{2.18}$$

The core velocities and pressure behave in a similar manner to (2.16)–(2.18) as we move into the upper boundary layer.

In the lower boundary layer, we write

$$\begin{aligned} y &= \epsilon^2 Y, \\ \boldsymbol{u}^* &= U_{\mathrm{m}}[(\epsilon^2 \lambda_0 Y, 0, 0) + (\epsilon^2 \tilde{u}, \epsilon^5 \tilde{v}, \epsilon^3 \tilde{w})\, E \ldots], \\ p^* &= \rho U_{\mathrm{m}}^2 [(\epsilon^4 \tilde{p}_0 + \epsilon^6 \tilde{q}_0 + \ldots]\, E, \end{aligned}$$

which, ignoring terms of $O(h^2)$, leads to the equations

$$\mathrm{i}\alpha \tilde{u} + \tilde{v}_Y + \tilde{w}_z = 0, \tag{2.19a}$$

$$\mathrm{i}(-\Omega + \alpha\lambda_0 Y)\, \tilde{u} + \lambda_0 \tilde{v} + \lambda_{0z} Y \tilde{w} = -\mathrm{i}\alpha \tilde{p}_0 + \tilde{u}_{YY}, \tag{2.19b}$$

$$\mathrm{i}(-\Omega + \alpha\lambda_0 Y)\, \tilde{w} = -\tilde{q}_{0z} + \tilde{w}_{YY}, \tag{2.19c}$$

$$\tilde{p}_0 = \text{const.}, \tag{2.19d}$$

$$\tilde{q}_0 = \tilde{q}_0(z), \tag{2.19e}$$

with boundary conditions

$$\tilde{u} = \tilde{v} = \tilde{w} = 0 \quad \text{on } Y = 0, \tag{2.20a}$$

$$\tilde{u} \to A_0, \quad \tilde{w} \to 0, \quad \tilde{p}_0 \to \hat{p}_0 \quad \text{as } Y \to \infty, \tag{2.20b}$$

$$\tilde{u}, \tilde{v}, \tilde{w}, \tilde{q}_0 \text{ periodic in } z. \tag{2.20c}$$

The scalings of $\tilde{u}$, $\tilde{v}$ and $\tilde{p}_0$ come from matching with the core whereas the scalings for $\tilde{w}$ and $\tilde{q}_0$ have been chosen as large as possible. These two terms will be driven by matching with higher-order terms in the core and are not specified uniquely by (2.19) and (2.20). Equations (2.19) are different from the usual linearized boundary-layer equations because the cross-flow (w) momentum equation is driven by a much smaller pressure term, q_0, than the streamwise u-momentum equation. The velocities generated by this small pressure are important at leading order because of the fast-z derivatives. Following Smith (1979*a*), (2.19*c*) can be solved for $\tilde{w}$ in terms of $\tilde{q}_0$,

$$\tilde{w} = \frac{\tilde{q}_{0z} M(\xi)}{(\mathrm{i}\alpha\lambda_0)^{\frac{2}{3}}}, \tag{2.21}$$

where

$$\left.\begin{aligned} M(\xi) &= \mathrm{Ai}(\xi) \int_{\xi_0}^{\xi} \frac{\mathrm{d}s}{\mathrm{Ai}^2(s)} \int_{\infty}^{s} \mathrm{Ai}(s_1)\, \mathrm{d}s_1, \\ \xi &= (\mathrm{i}\alpha\lambda_0)^{\frac{1}{3}} \left(y - \frac{\Omega}{\alpha\lambda_0}\right), \quad \xi_0 = \frac{-\mathrm{i}^{\frac{1}{3}}\Omega}{(\alpha\lambda_0)^{\frac{2}{3}}}, \end{aligned}\right\} \tag{2.22}$$

and Ai is the Airy function that satisfies $\mathrm{Ai}'' = \xi\,\mathrm{Ai}$. Eliminating $\tilde{v}$ between (2.19a) and (2.19b) by differentiating (2.19b), substituting for $\tilde{w}$ from (2.21) and solving for $\tilde{u}$ we get

$$(\mathrm{i}\alpha\lambda_0)^{\frac{5}{3}}\tilde{u}_\xi = -\lambda_0\tilde{q}_{0zz}M'(\xi)+\tfrac{1}{3}\lambda_{0z}\tilde{q}_{0z} \times\left\{3M'(\xi)+\tfrac{1}{2}M''''(\xi)-2\mathrm{Ai}'(\xi)\left[\frac{\xi_0 M'(\xi_0)}{\mathrm{Ai}\,(\xi_0)}\right]\right\}+B\,\mathrm{Ai}\,(\xi), \quad (2.23)$$

where the constant B is determined by the outer boundary condition on $\tilde{u}$ in (2.20),

$$\left.\begin{aligned} B &= (\mathrm{i}\alpha\lambda_0)^{\frac{5}{3}}\frac{A_0}{K(\xi_0)}-\tfrac{1}{2}\lambda_{0z}\tilde{q}_{0z}\xi_0\frac{M'(\xi_0)}{K(\xi_0)},\\ K(\xi_0) &= \int_{\xi_0}^{\infty}\mathrm{Ai}\,(\xi)\,\mathrm{d}\xi. \end{aligned}\right\} \quad (2.24)$$

From matching with the core $\tilde{p}_0 = \hat{p}_0$ and putting $Y = 0$ in (2.19b) and using (2.23) and (2.24), we get an expression for $\tilde{p}_0$ in terms of $\tilde{q}_0$ and A_0. Substituting for A_0 from (2.18) gives

$$\left.\begin{aligned} \tilde{q}_{0zz}+\psi_0\tilde{q}_{0z} &= \alpha^2\tilde{p}_0+\tfrac{1}{2}(\hat{p}_1-\hat{p}_0)\,\phi_{yyy}|_{y=0}\frac{\mathrm{Ai}'(\xi_0)}{(\mathrm{i}\alpha\lambda_0)^{\frac{1}{3}}K(\xi_0)},\\ \psi_0 &= -\frac{\lambda_{0z}}{\lambda_0}\left(\frac{3}{2}+\frac{\xi_0}{2\,\mathrm{Ai}\,(\xi_0)}[\xi_0 K(\xi_0)+\mathrm{Ai}'(\xi_0)]\right). \end{aligned}\right\} \quad (2.25)$$

The problem in the upper critical layer at $y = 1$ is the same as that at $y = 0$ with $(\lambda_1(z), A_1, \tilde{p}_1, \tilde{q}_1, \hat{p}_1)$ instead of $(\lambda_0(z), A_0, \tilde{p}_0, \tilde{q}_0, \hat{p}_0)$ in (2.19)–(2.24), and with (2.18) replaced by

$$(\mathrm{i}\alpha)^2\lambda_1 A_1 = -\tfrac{1}{2}(\hat{p}_1-\hat{p}_0)\,\phi_{yyy}|_{y=1}. \quad (2.26)$$

This leads to

$$\left.\begin{aligned} \tilde{q}_{1zz}+\psi_1\tilde{q}_{1z} &= \alpha^2\hat{p}_1+\tfrac{1}{2}(\hat{p}_0-\hat{p}_1)\,\phi_{yyy}|_{y=1}\frac{\mathrm{Ai}'(\xi_1)}{(\mathrm{i}\alpha\lambda_1)^{\frac{1}{3}}K(\xi_1)},\\ \psi_1 &= -\frac{\lambda_{1z}}{\lambda_1}\left\{\frac{3}{2}+\frac{\xi_1}{2\,\mathrm{Ai}\,(\xi_1)}[\xi_1 K(\xi_1)+\mathrm{Ai}'(\xi_1)]\right\},\\ \xi_1 &= -\frac{\mathrm{i}^{\frac{1}{3}}\Omega}{(\alpha\lambda_1)^{\frac{2}{3}}}. \end{aligned}\right\} \quad (2.27)$$

In the limit as $\partial/\partial z \to O(Re^{-\frac{1}{7}})$, $\tilde{q}_0$, and $\tilde{q}_1$ would tend to $\tilde{p}_0$ and $\tilde{p}_1$ so that (2.25) and (2.27) would become the coupled second-order differential equations of Smith (1979a). Our equations as they stand are easier to deal with as they are only first-order differential equations in $\tilde{q}_{0z}$ and $\tilde{q}_{1z}$. Integrating (2.25) once and using the periodicity condition (2.20c) gives

$$0 = \hat{p}_0\alpha^2\int_0^{2\pi/k}\exp\left[\int_0^z\psi_0(z_1)\,dz_1\right]\mathrm{d}z + (\hat{p}_1-\hat{p}_0)\frac{1}{2}\int_0^{2\pi/k}\left[\exp\left[\int_0^z\psi_0(z_1)\,\mathrm{d}z_1\right]\phi_{yyy}|_{y=0}\frac{\mathrm{Ai}'(\xi_0)}{(\mathrm{i}\alpha\lambda_0)^{\frac{1}{3}}K(\xi_0)}\,\mathrm{d}z.$$

Integrating (2.27) gives a similar equation for $\hat{p}_0$ and $\hat{p}_1$ involving ξ_1, and on eliminating $\hat{p}_0$ and $\hat{p}_1$ from these two equations we obtain

$$2\alpha^2 = \frac{\displaystyle\int_0^{2\pi/k} \exp\left[\int_0^z \psi_0\,\mathrm{d}z_1\right] \frac{\mathrm{Ai}'(\xi_0)}{(\mathrm{i}\alpha\lambda_0)^{\frac{1}{3}}K(\xi_0)}\phi_{yyy}|_{y=0}\,\mathrm{d}z}{\displaystyle\int_0^{2\pi/k} \exp\left[\int_0^z \psi_0\,\mathrm{d}z_1\right]\mathrm{d}z} + \frac{\displaystyle\int_0^{2\pi/k} \exp\left[\int_0^z \psi_1\,\mathrm{d}z_1\right] \frac{\mathrm{Ai}'(\xi_1)}{(\mathrm{i}\alpha\lambda_1)^{\frac{1}{3}}K(\xi_1)}\phi_{yyy}|_{y=1}\,\mathrm{d}z}{\displaystyle\int_0^{2\pi/k} \exp\left[\int_0^z \psi_1\,\mathrm{d}z_1\right]\mathrm{d}z}. \tag{2.28}$$

This is the dispersion relation or eigenrelation, giving α in terms of Ω for high-Reynolds-number, linear Tollmien–Schlichting waves. It applies to any unidirectional flow $(\bar{U}(y,z),0,0)$ so long as the period of the z-variation $2\pi/k \ll Re^{\frac{1}{7}}$. Thus the eigenrelation is also applicable to high-Reynolds-number flows in pipes of finite cross-section. Here z would correspond to distance measured around the pipe.

Three stages are needed to work out values of (α,Ω) on the curve given by (2.28) for the Taylor-vortex case $\bar{U} = U_0 + u$:

(i) First, for a given Taylor number T we must find a steady solution of (2.2)–(2.4) and hence $\bar{U}$;

(ii) Once $\bar{U}$ is known we can determine the core pressure ϕ by solving (2.13) and (2.15);

(iii) Finally we can solve (2.28) with ξ_0, ψ_0, ξ_1 and ψ_1 given by (2.22), (2.25) and (2.27) and λ_0 and λ_1 given by

$$\lambda_0 = \bar{U}_y|_{y=0}, \quad \lambda_1 = -\bar{U}_y|_{y=1}.$$

3. Weakly nonlinear theory

In order to find nonlinear solutions of the vortex equations (2.2)–(2.5), we need to use a numerical method, as in §5. However, when the Taylor number is only slightly greater than the critical linear Taylor number T_c, the amplitude of the vortices is small and solutions of (2.2)–(2.5) are described by the weakly nonlinear theory of Seminara (1976). We now apply our dispersion relation (2.28) to Seminara's velocity profile. The results we obtain indicate how the stability of the flow is affected when the flow becomes slightly three-dimensional and will provide a useful check on the full nonlinear calculations of §5. The weakly nonlinear velocity in the streamwise direction is given by

$$\bar{U} = U_0 + \Delta u_1 \cos kz + \Delta^2(u_{20} + u_{22}\cos 2kz) + O(\Delta^3). \tag{3.1}$$

Here the vortex wavenumber k is the critical one for linear vortices, $k = k_c = 3.951$, and the vortex amplitude Δ is related to the Taylor number by

$$\Delta = 0.1725\left(\frac{T-T_c}{T_c}\right)^{\frac{1}{2}} \ll 1. \tag{3.2}$$

The velocities u_1, u_{20} and u_{22} are given by Seminara (1976) and are independent of z.

The solution of the pressure equation (2.13) with boundary conditions (2.15) is then forced to behave in a similar manner to (3.1):

$$\phi = \phi_0 + \Delta\phi_1 \cos kz + \Delta^2(\phi_{20} + \phi_{22}\cos 2kz) + O(\Delta^3). \tag{3.3}$$

Here we are only interested in the leading-order effects of the vortex on the dispersion relation. Since the integral of $\cos kz$ over a period is zero, the fundamental $O(\Delta)$-terms will only appear as a product with other $O(\Delta)$-terms and so will only have an $O(\Delta^2)$ effect. Hence we must also take into account the mean flow correction terms u_{20} and ϕ_{20}. By a similar argument the first-harmonic terms $O(\Delta^2)\cos 2kz$ will only have an $O(\Delta^3)$ effect, and so are ignored here. Substituting (3.3) into (2.13) we find that the pressure term ϕ can be found from the following:

$$\left.\begin{aligned} \phi_0 &= 6y^5 - 15y^4 + 10y^3, \\ \phi_{20y} &= 5(\tfrac{1}{3}U_0 u_{20} - \tfrac{1}{4}u_1^2) + \phi_{1y}\frac{u_1}{u_0} - \tfrac{5}{6}CU_0^2, \\ \text{where} \quad C &= \int_0^1 \left(5(\tfrac{1}{3}U_0 u_{20} - \tfrac{1}{4}u_1^2) + \phi_{1y}\frac{u_1}{U_0}\right)\mathrm{d}y, \end{aligned}\right\} \tag{3.4}$$

and that the fundamental pressure term ϕ_1 is governed by

$$\left(\frac{\phi_{1y}}{U_0^2}\right)_y - \frac{k^2\phi_1}{U_0^2} = \frac{5}{3}\left(\frac{u_1}{U_0}\right)_y, \quad \phi_1 = 0 \quad \text{at } y = 0, 1. \tag{3.5}$$

If we write the skin friction at the walls as

$$\lambda_0 = \bar{U}_y|_{y=0} = 6 + \Delta\mu_1 \cos kz + \Delta^2(\mu_{20} + \ldots), \tag{3.6a}$$

$$\lambda_1 = -\bar{U}_y|_{y=0} = 6 + \Delta\nu_1 \cos kz + \Delta^2(\nu_{20} + \ldots), \tag{3.6b}$$

then from (3.4) the pressure terms we need to evaluate the dispersion relation are

$$\left.\begin{aligned} \phi_{0yyy}|_{y=0} &= \phi_{0yyy}|_{y=1} = 60, \\ \phi_{20yyy}|_{y=0} &= 20\mu_{20} - \tfrac{5}{2}\mu_1^2 + \phi_{1yyy}|_{y=0}\tfrac{1}{6}\mu_1 - 60C, \\ \phi_{20yyy}|_{y=1} &= 20\nu_{20} - \tfrac{5}{2}\nu_1^2 + \phi_{1yyy}|_{y=1}\tfrac{1}{6}\nu_1 - 60C. \end{aligned}\right\} \tag{3.7}$$

We can define a mean value for ξ_0, ξ_1 by writing

$$\bar{\xi} = \frac{-\Omega\, \mathrm{e}^{\mathrm{i}\pi/6}}{(6\alpha)^{\frac{2}{3}}}, \tag{3.8}$$

and substituting (3.6a) into the definition of ψ_0, (2.25), we find after some simplification that the integrating factor in (2.28) becomes

$$\exp\left[\int_0^z \psi_0\, \mathrm{d}z_1\right] \sim \frac{1}{6^{\frac{2}{3}}}[1 - \tfrac{1}{12}\Delta\mu_1 G\cos kz + O(\Delta^2)], \tag{3.9a}$$

where

$$G = 3 + \frac{\bar{\xi}}{\mathrm{Ai}(\bar{\xi})}(\bar{\xi}K + \mathrm{Ai}'). \tag{3.9b}$$

Also, the rest of the integrand in the eigenrelation can be written as

$$\frac{\mathrm{Ai}'(\xi_0)}{K(\xi_0)(\mathrm{i}\alpha\lambda_0)^{\frac{1}{3}}} \sim \frac{1}{(6\mathrm{i}\alpha)^{\frac{1}{3}}}\frac{\mathrm{Ai}'(\bar{\xi})}{K(\bar{\xi})}[1 - \tfrac{1}{18}\Delta\mu_1 F_1\cos kz + \Delta^2(\tfrac{1}{36}\mu_1^2 F_2 - \tfrac{1}{18}\mu_{20}F_1)], \tag{3.10a}$$

where
$$F_1 = 2\frac{\bar{\xi}\,\mathrm{Ai}\,(\bar{\xi})}{K(\bar{\xi})\,\mathrm{Ai}'\,(\bar{\xi})}(\bar{\xi}K + \mathrm{Ai}') + 1, \tag{3.10b}$$

and
$$9F_2 = 1 + \bar{\xi}^2\frac{\mathrm{Ai}}{\mathrm{Ai}'} + \frac{\bar{\xi}}{K}(\bar{\xi}K + \mathrm{Ai}')\left(\bar{\xi} + \frac{7}{2}\frac{\mathrm{Ai}}{\mathrm{Ai}'} + 2\bar{\xi}\frac{\mathrm{Ai}^2}{K\,\mathrm{Ai}'}\right). \tag{3.10c}$$

Combining these results we can evaluate the part of (2.28) corresponding to the lower boundary layer:

$$\frac{\int_0^{2\pi/k} \exp\left[\int_0^z \psi_0\,\mathrm{d}z_1\right] \frac{\mathrm{Ai}'\,(\xi_0)}{(\mathrm{i}\alpha\lambda_0^{\frac{1}{3}}K(\xi_0)}\phi_{yyy}|_{y=0}\,\mathrm{d}z}{\int_0^{2\pi/k} \exp\left[\int_0^z \psi_0\,\mathrm{d}z_1\right]\mathrm{d}z}$$

$$\sim \frac{\mathrm{Ai}'(\bar{\xi})}{K(\bar{\xi})}\frac{60}{(6\mathrm{i}\alpha)^{\frac{1}{3}}}\left\{1 + \Delta^2\left[\tfrac{1}{36}\mu_1^2(F_2 + \tfrac{1}{12}F_1 G - \tfrac{3}{2}) - \tfrac{1}{6}\mu_{20}(\tfrac{1}{3}F_1 - 2)\right.\right.$$

$$\left.\left. - \frac{\phi_{1yyy}|_{y=0}\mu_1(\frac{1}{6}F_1 + \frac{1}{4}G - 1)}{360} - C\right]\right\}.$$

Using a similar result for the other half of (2.28), we get the following eigenrelation:

$$\frac{(6\mathrm{i}\alpha)^{\frac{1}{3}}\alpha^2 K(\bar{\xi})}{60\mathrm{Ai}'(\bar{\xi})} = 1 + \tfrac{1}{2}\Delta^2\left(\frac{\mu_1^2 + \nu_1^2}{36}(F_2 + \tfrac{1}{12}F_1 G - \tfrac{3}{2})\right.$$

$$\left. + \frac{(\mu_1\phi_{1yyy}|_{y=0} + \nu_1\phi_{1yyy}|_{y=-1})(1 - \frac{1}{6}F_1 - \frac{1}{4}G)}{360} - 2C\right), \tag{3.11}$$

where we have used the result $\mu_{20} + \nu_{20} = 0$.

This can be simplified further by writing

$$\alpha = \alpha_0 + \Delta^2\alpha_1, \quad \bar{\xi}_0 = \frac{-\Omega\,\mathrm{e}^{\mathrm{i}\pi/6}}{(6\alpha_0)^{\frac{2}{3}}},$$

where α_0 and $\bar{\xi}_0$ satisfy the channel-flow eigenrelation

$$\frac{(6\mathrm{i}\alpha_0)^{\frac{1}{3}}\alpha_0^2 K(\bar{\xi}_0)}{60\mathrm{Ai}'\,(\bar{\xi}_0)} = 1,$$

valid when $\Delta = 0$. In this case (3.11) reduces to

$$\frac{\alpha_1}{\alpha_0} = \frac{3}{2}\left\{\frac{\mu_1^2 + \nu_1^2}{36}(F + \tfrac{1}{12}F_1 G - \tfrac{3}{2})\right.$$

$$\left. + \frac{(\mu_1\phi_{1yyy}|_{y=0} + \nu_1\phi_{1yyy}|_{y=-1})(1 - \frac{1}{6}F_1 - \frac{1}{4}G)}{360} - 2C\right\}(F_1 + 6)^{-1}, \tag{3.12}$$

where F_1, F_2 and G are now evaluated at $\xi = \bar{\xi}_0$ instead of $\bar{\xi}$.

The constants in (3.12) are obtained from Seminara (1976) and by solving (3.5):

$$\frac{\mu_1^2 + \nu_1^2}{36} = 8.072,$$

$$(\mu_1\phi_{1yyy}|_{y=0} + \nu_1\phi_{1yyy}|_{y=-1}) = 6.843,$$

$$-2C = 26.86.$$

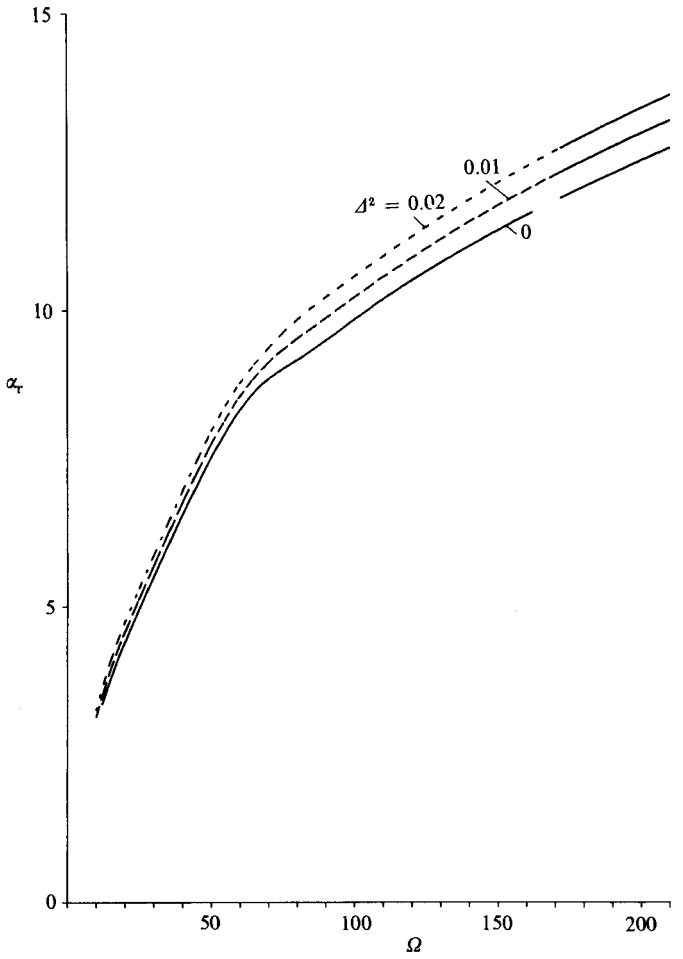

FIGURE 1. The wavenumber predicted by the weakly nonlinear theory and corresponding asymptotic results for large values of Ω.

We now choose to look only at the spatial stability of the vortex motion; that is for a given real frequency Ω we solve (3.12) numerically to find the wavenumber. If α_i, the imaginary part of the wavenumber, turns out to be positive, then the resulting waves decay downstream as $x \to \infty$, whilst if $\alpha_i < 0$ the waves will grow exponentially.

Figures 1 and 2 show α_r and α_i plotted against Ω for $A^2 = 0$, 0.01, 0.02 corresponding to Taylor numbers of $T = T_c$, $1.33T_c$, $1.67T_c$. The general pattern is the same in all three cases. For the frequency less than some critical value Ω_c (depending on the Taylor number), all disturbances decay. At $\Omega = \Omega_c$, $\alpha_i = 0$ so that linear disturbances neither grow nor decay. This point corresponds to the asymptotic limit of the lower branch of the neutral curve. For $\Omega > \Omega_c$ all waves grow and, as $\Omega \to \infty$, (α_i) decays to zero since we are tending towards the upper branch of the neutral curve. Disturbances corresponding to the upper branch occur on different length- and timescales to the lower-branch disturbances, so that in an analysis near the upper branch x and t would be scaled on different powers of the Reynolds number to (2.7). Thus however large Ω is we shall never actually reach the upper branch where $\alpha_i = 0$. The results of figure 2 show that the vortices have negligible effect on the

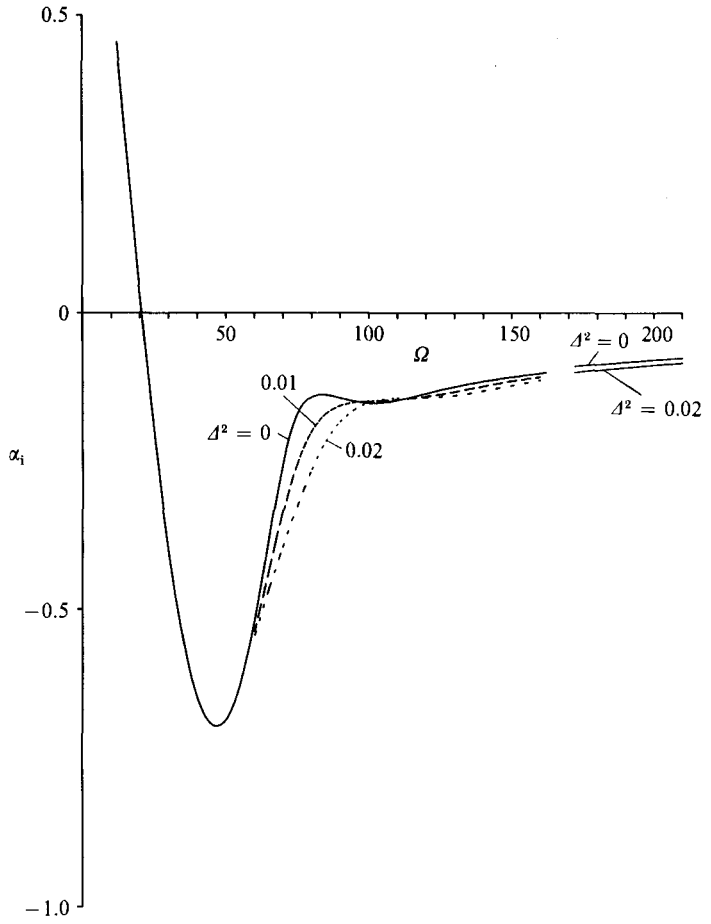

FIGURE 2. The growth rates predicted by the weakly nonlinear theory and the corresponding asymptotic results for large values of Ω.

neutral frequency Ω_c and that the growth rate over a band of frequencies is significantly increased. This corresponds to a destabilization of Poiseuille flow by the vortices. We shall see that this trend is also found when the fully nonlinear problem is solved numerically.

4. The high-frequency limit, $\Omega \to \infty$

In this section we determine the asymptotic behaviour of the eigenrelation (2.28) when $\Omega \to \infty$. The result we obtain, (4.9), is a generalization of the standard behaviour of high-frequency waves in a channel. We assume that $\Omega/\alpha^{\frac{2}{3}} \to \infty$ as $\Omega \to \infty$, which means that ξ_0 and $\xi_1 \to \infty$. This can be checked at the end of the calculation. First we need two results giving the behaviour of the Airy function, its derivative, and its integral for large arguments. Writing $\mathrm{Ai}(s) = \mathrm{Ai}''/s$ and integrating by parts, we find

$$K(\xi) = \int_\xi^\infty \mathrm{Ai}(s)\,\mathrm{d}s \sim -\frac{\mathrm{Ai}'(\xi)}{\xi} - \frac{\mathrm{Ai}}{\xi^2} - \frac{2\mathrm{Ai}'}{\xi^4} + \ldots \quad \text{as } \xi \to \infty. \tag{4.1}$$

Also it is known (see e.g. Abramowitz & Stegun 1965) that the ratio of the Airy function to its derivative is given by

$$\frac{\mathrm{Ai}}{\mathrm{Ai}'} \sim -\xi^{-\frac{1}{2}} \quad \text{as } \xi \to \infty. \tag{4.2}$$

Using these two results we can calculate the asymptotic behaviour of each term in (2.28). So from (2.25) using (4.1) and (4.2) we get

$$\psi_0 \sim -\frac{\lambda_{0z}}{\lambda_0}\left(1+\frac{1}{\xi^{\frac{3}{2}}}+\ldots\right) \quad \text{as } \xi \to \infty,$$

and using (2.22) we can write this as

$$\psi_0 \sim -\frac{\lambda_{0z}}{\lambda_0} - \frac{\lambda_{0z}\alpha}{(-\mathrm{i}\Omega^3)^{\frac{1}{2}}}.$$

Hence the integrating factor

$$\exp\left[\int_0^z \psi_0 \,\mathrm{d}z\right] \sim \frac{1}{\lambda_0}\left(1-\frac{\lambda_0\alpha}{(-\mathrm{i}\Omega^3)^{\frac{1}{2}}}+\ldots\right) \quad \text{as } \xi \to \infty, \tag{4.3}$$

so that

$$\int_0^{2\pi/k} \exp\left[\int_0^z \psi_0 \,\mathrm{d}z\right]\mathrm{d}z \sim \int_0^{2\pi/k} \frac{\mathrm{d}z}{\lambda_0} - \frac{2\pi}{k}\frac{\alpha}{(-\mathrm{i}\Omega^3)^{\frac{1}{2}}} \quad \text{as } \xi \to \infty. \tag{4.4}$$

Also from (4.1) and (4.2)

$$\frac{\mathrm{Ai}'(\xi_0)}{K(\xi_0)} \sim -\xi_0\left(1+\frac{1}{\xi_0^{\frac{3}{2}}}+\ldots\right) = -\xi_0\left(1+\frac{\lambda_0\alpha}{(-\mathrm{i}\Omega^3)^{\frac{1}{2}}}+\ldots\right). \tag{4.5}$$

Combining this with (4.3) gives

$$\frac{\exp\left[\int_0^z \psi_0 \,\mathrm{d}z\right]\mathrm{Ai}'(\xi_0)}{K(\xi_0)(\mathrm{i}\alpha\lambda_0)^{\frac{1}{3}}} \sim \frac{\Omega}{\alpha\lambda_0^2}. \tag{4.6}$$

Substituting (4.4) and (4.6) together with similar expressions involving ξ, into the dispersion relation (2.28), we obtain

$$2\alpha^2 \to \frac{\Omega}{\alpha}\left\{\frac{\Phi_0}{L_0-\dfrac{2\pi\alpha}{k(-\mathrm{i}\Omega^3)^{\frac{1}{2}}}}+\frac{\Phi_1}{L_1-\dfrac{2\pi\alpha}{k(-\mathrm{i}\Omega^3)^{\frac{1}{2}}}}\right\}, \tag{4.7}$$

where

$$\Phi_i = \int_0^{2\pi/k} \frac{\phi_{yyy}}{\lambda_i^2}\bigg|_{y=i} \mathrm{d}z, \quad L_i = \int_0^{2\pi/k} \frac{\mathrm{d}z}{\lambda_i}, \quad i = 0, 1. \tag{4.8}$$

We can now obtain an asymptotic series for α in inverse powers of Ω from (4.7) in the form

$$\alpha \sim C_1\Omega^{\frac{1}{3}} - \mathrm{e}^{\mathrm{i}\pi/4}C_2\Omega^{-\frac{5}{6}}, \tag{4.9}$$

where

$$C_1^3 = \frac{1}{2}\left(\frac{\Phi_0}{L_0}+\frac{\Phi_1}{L_1}\right), \quad C_2 = \frac{\pi}{3kC_1}\left(\frac{\Phi_0}{L_0^2}+\frac{\Phi_1}{L_1^2}\right).$$

(We note here that $\Omega \to \infty$ implies that $\xi_0, \xi_1 \to \infty$ as assumed earlier.)

Thus the imaginary part of α decays to zero like some constant times $\Omega^{-\frac{5}{6}}$. The actual value of this constant depends on the vortex profile through the constants C_1 and C_2. We now determine these constants for vortices governed by the weakly nonlinear theory described in §3. If the velocity is given by (3.1), we find that

$$\Phi_i = \frac{2\pi}{k}\tfrac{5}{3}(1-\Delta^2 C), \quad i = 0, 1,$$

and

$$L_1 = \frac{2\pi}{6k}(1+\Delta^2(\tfrac{1}{72}\mu_1^2 - \tfrac{1}{6}\mu_{20})),$$

with a similar formula for L_2 but with ν replacing μ. Hence

$$C_1^3 = 10\left(1-\Delta^2\left(C+\frac{1}{4}\frac{(\mu_1^2+\nu_1^2)}{36}\right)\right),$$

$$C_2 = \frac{20}{C_1}\left(1-\tfrac{1}{2}\Delta^2\left(2C+\frac{\mu_1^2+\nu_1^2}{36}\right)\right),$$

so that the asymptotic form for the growth rate is given by

$$-\alpha_i \sim \sqrt{2}\,(10^{\frac{2}{3}})\left(1-\tfrac{1}{6}\Delta^2\left[4C+\frac{5}{2}\left(\frac{\mu_1^2+\nu_1^2}{36}\right)\right]\right)\Omega^{-\frac{5}{6}}. \tag{4.10}$$

This asymptote is plotted in figure 2 for various values of Δ along with the corresponding weakly nonlinear dispersion relations. The asymptotic form (4.10) is seen to accurately predict α_i over a wide range of frequencies and thus provides a useful check on the calculations of §3.

5. The numerical calculation of a finite-amplitude Taylor vortex

Here we describe how we integrated (2.3) numerically to find the finite-amplitude Taylor vortex whose instability we wish to determine. The method used is essentially that described by Rogers & Beard (1969) who investigated numerically the classical Taylor problem driven by the motion of the inner cylinder. Rogers & Beard solved a system similar to (2.3) by Fourier expanding u and v in the z-direction and using finite differences in the radial direction. Later Fasel & Booz (1984) performed related calculations using finite differences in both directions. The method of the latter authors is apparently the most efficient at very high Taylor numbers where jet-like structures develop along the cylinders. Here we do not perform calculations at such high Taylor numbers, so we use the method of Rogers & Beard.

Thus the velocity components in (2.3) are expanded as

$$\left.\begin{aligned} u &= u_0 + \sum_1^\infty u_n(y,t)\cos knz, \\ v &= \sum_1^\infty v_n(y,t)\cos knz, \\ w &= \sum_1^\infty w_n(y,t)\sin knz. \end{aligned}\right\} \tag{5.1}$$

Here we have anticipated the usual result that the only mean flow generated by the vortex is in the streamwise direction. The expansions (5.1) are then substituted into (2.3), and the coefficients of $\cos knz$ are equated to give an infinite sequence of

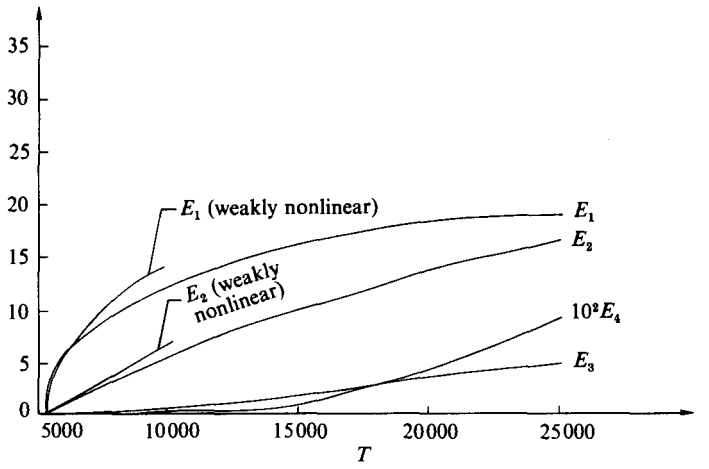

FIGURE 3. The functions E_1, E_2, E_3, E_4 at different Taylor numbers.

coupled nonlinear differential equations for $\{u_n\}$ and $\{v_n\}$. Thus for example the equation for u_0 is

$$\frac{\partial u_0}{\partial t} - \frac{\partial^2 u_0}{\partial y^2} = \frac{1}{4} \sum_{j=1}^{\infty} (u_j v_j)_y. \tag{5.2}$$

We obtain steady-state solutions of (2.3) by integrating forward in time from some appropriate initial guess. At Taylor numbers close to the critical, the initial guess can be taken to be the weakly nonlinear state described in §4. At high Taylor numbers the initial guess was taken to be the equilibriated solution from a previous calculation at a lower Taylor number.

A fully implicit scheme was used to march forward in time. Hence if Δt is the time step and h the step length in the y-direction we obtain a stable scheme for $\Delta t \sim O(h)$. The nonlinear terms on the right-hand side of the disturbance equations were always evaluated explicitly. The number of Fourier modes and intervals in the y-direction required to achieve a solution sufficiently accurate for our purpose depends on the ratio T/T_c. In order to monitor the energy in different harmonics, we followed Rogers & Beard and defined

$$E_q = \left\{ \int_0^1 v_q^2 \, dy \right\}^{\frac{1}{2}}, \quad F_q = \left\{ \int_0^1 u_q^2 \, dy \right\}^{\frac{1}{2}}. \tag{5.3}$$

The number of axial modes required was varied until the converged values of E_q, F_q achieved sufficient accuracy. Similarly the step length h was varied until E_q, F_q converged to sufficiently accurate values. For the calculations reported here, it was found that eight axial modes and $h = 0.01$ were sufficient to enable us to determine the dispersion relation to the accuracy indicated in §7. In figures 3 and 4, we show the dependence of E_q and F_q on T for $k = k_c = 3.951$, the most dangerous Taylor-vortex mode. We see that at sufficiently small values of $\{T/T_c - 1\}$ the results are consistent with the weakly nonlinear results which can be derived from Seminara (1976).

Once the Taylor vortex has been computed, the wavenumber $\alpha(\Omega, T)$ can be calculated using the procedure outlined at the end of §2. The functions required in the calculation were evaluated from the series or asymptotic expansion of Ai depending on the size of the argument. The wave-flow equation (2.13) was solved by a finite-difference method together with an iteration procedure to evaluate the

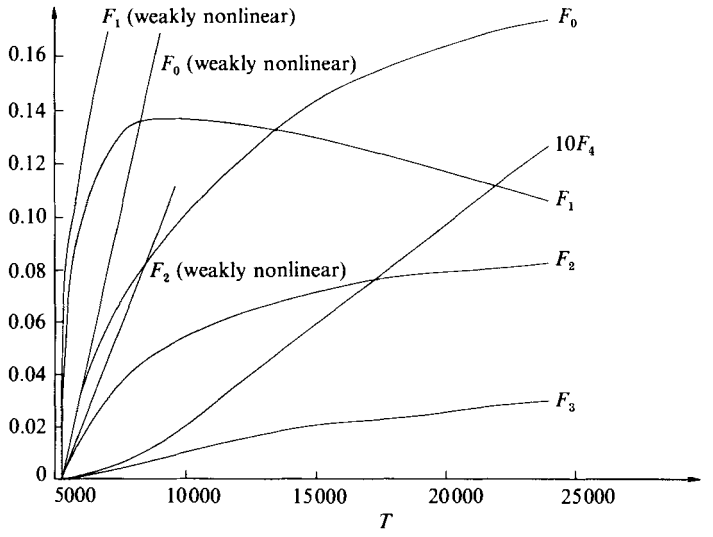

FIGURE 4. The functions F_0, F_1, F_2, F_3, F_4 at different Taylor numbers.

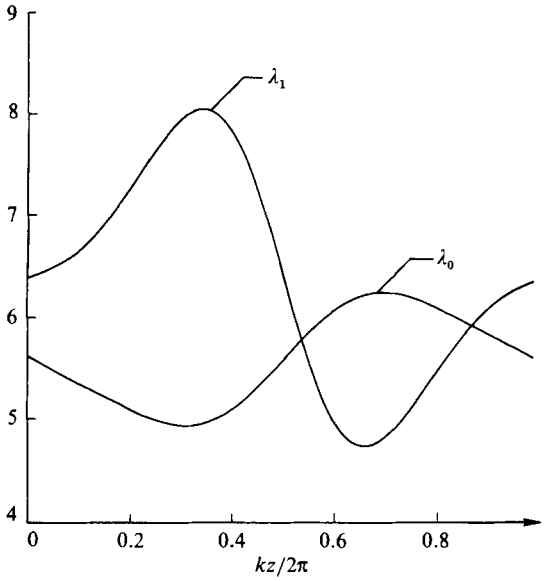

FIGURE 5. The shear stresses λ_0 and λ_1 as functions of z for $T = 11000$, $k = 3.951$.

terms involving z-derivatives. In figures 5 and 6, we have shown the functions $\lambda_0(z)$, $\lambda_1(z)$, $\phi_{yyy}(0,z)$, $\phi_{yyy}(1,z)$ obtained from such a calculation at $T = 11000$. We recall that at $T = T_c$, $\lambda_0 = \lambda_1 = 6$, $\phi_{yyy}(0,z) = \phi_{yyy}(1,z) = 60$ so that even at about twice the critical Taylor number the vortices have a significant effect on the wave-flow problem. The integrals in (2.28) were evaluated by solving ordinary differential equations related to (2.25) and (2.27) rather than performing the double integrations numerically. We postpone until §7 a discussion of the results obtained at higher Taylor numbers. The calculation of the finite-amplitude Taylor vortex beyond $T \sim 27000$ was not possible because it is apparently unstable to another Taylor-vortex mode with wavenumber $2k_c$. The mode could of course be found for $T > 28000$ by solving the steady-state equations, but such a calculation was not carried out.

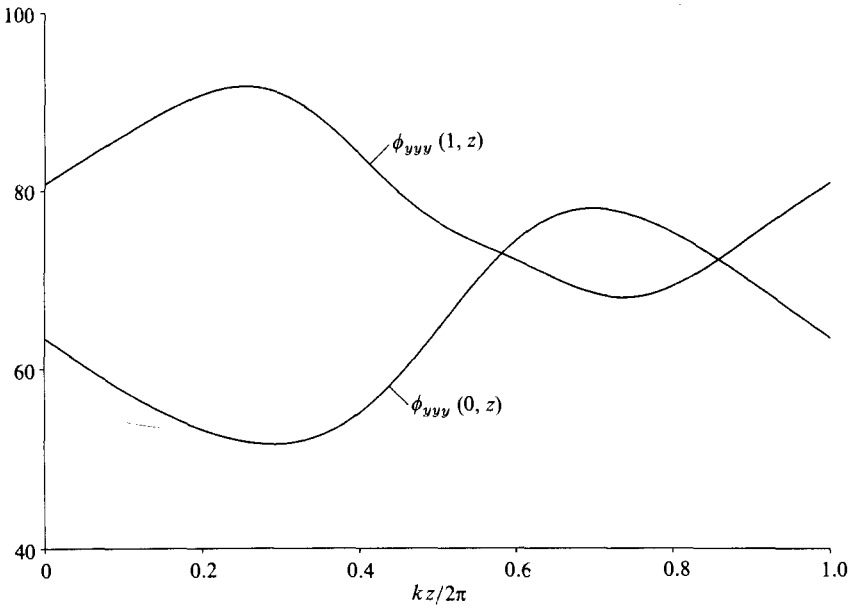

FIGURE 6. The functions $\phi_{yyy}(0,z)$, $\phi_{yyy}(1,z)$ for $T = 11000$, $k = 3.951$.

6. Oblique waves

The method used to obtain the dispersion relation in §2 can be extended to deal with Tollmien–Schlichting waves travelling at an angle to the main direction of flow of the Taylor–Görtler vortex. In this case, the perturbation velocities and pressure will depend on the slow Tollmien–Schlichting cross-stream coordinate ϵz, as well as the relatively fast vortex coordinate z. In the boundary layer, this forces a much larger pressure gradient in the z-direction which alters the structure of the flow there.

In the core, then, the perturbation scalings (2.8) remain the same, but (2.9) is changed to

$$E = h \exp(\mathrm{i}(\alpha X + \beta \epsilon z - \Omega \tilde{T})), \quad h \ll 1. \tag{6.1}$$

This leaves the core-flow problem (2.10*a–d*) unchanged and leads to the same matching conditions (2.16) and (2.17). However, because of the z-dependence in (6.1), the pressure gradient has a component in the z-direction of $O(\epsilon^5)$ in the boundary layer, as opposed to $O(\epsilon^6)$ beforehand. This then forces the following new scalings in the boundary layer:

$$y = \epsilon^2 Y, \quad p^* = \rho U_{\mathrm{m}}^2[\epsilon^4 p_0 + \epsilon^5 p_1(z) + \epsilon^6 p_2(z) + \ldots]E,$$
$$\boldsymbol{u}^* = U_{\mathrm{m}}[(\epsilon^2 \lambda_0 Y, 0, 0) + (\epsilon u_0 + \epsilon^2 u_1 + \ldots, \epsilon^4 v_0 + \epsilon^5 v_1 + \ldots, \epsilon^2 w_0 + \epsilon^3 w_1 + \ldots)E].$$

Substituting the above into the Navier–Stokes equations and linearizing, we obtain the following two sets of equations:

$$\left.\begin{aligned}
&\mathrm{i}\alpha u_0 + v_{0Y} + w_{0z} = 0, && (6.2a)\\
&\mathrm{i}(-\Omega + \alpha\lambda_0 Y)u_0 + \lambda_0 v_0 + \lambda_{0z} Y w_0 = u_{0YY}, && (6.2b)\\
&\mathrm{i}(-\Omega + \alpha\lambda_0 Y)w_0 = -\mathrm{i}\beta p_0 - p_{1z} + w_{0YY}, && (6.2c)\\
&u_0 = v_0 = w_0 = 0 \quad \text{on } Y = 0, && (6.2d)\\
&u_0, w_0, \to 0, \quad p_0 = \hat{p}_0 \quad \text{as } Y \to \infty, && (6.2e)
\end{aligned}\right\}$$

and

$$\left.\begin{aligned} &\mathrm{i}\alpha u_1 + v_{1Y} + w_{1z} + \mathrm{i}\beta w_0 = 0, && (6.3a)\\ &\mathrm{i}(-\Omega + \alpha\lambda_0 Y)\,u_1 + \lambda_0 v_1 + \lambda_{0z} Y w_1 = -\mathrm{i}\alpha p_0 + u_{1YY}, && (6.3b)\\ &\mathrm{i}(-\Omega + \alpha\lambda_0 Y)\,w_1 = -\mathrm{i}\beta p_1 - p_{2z} + w_{1YY}, && (6.3c)\\ &u_1 = v_1 = w_1 = 0 \quad \text{on } Y = 0, && (6.3d)\\ &u_1 \to A_0, \quad w_1 \to 0 \quad \text{as } Y \to \infty. && (6.3e) \end{aligned}\right\}$$

Here we have ignored terms of $O(h^2)$ and $O(h^2/\epsilon)$; the latter of the two terms makes the extension of this work into the weakly nonlinear region non-trivial.

Equations (6.2) are the same as (2.19) and (2.20) with $(\tilde{u}, \tilde{v}, \tilde{w})$ replaced by (u_0, v_0, w_0) and $(\mathrm{i}\alpha\tilde{p}_0, \tilde{q}_{0z}, \tilde{A}_0)$ replaced by $(0, i\beta p_0 + p_{1z}, 0)$. Hence (6.2) can be reduced to the equivalent of (2.25):

$$(p_{1z} + \mathrm{i}\beta p_0)_z + \psi_0 (p_{1z} + \mathrm{i}\beta p_0) = 0.$$

For periodic solutions we have

$$p_{1z} = -\mathrm{i}\beta p_0 \left(1 - \frac{2\pi}{k} \frac{\exp\left[-\int_0^z \psi_0 \, \mathrm{d}z_1 \right]}{\int_0^{2\pi/k} \exp\left[-\int_0^z \psi_0 \, \mathrm{d}z_1 \right] \mathrm{d}z} \right). \tag{6.4}$$

By adding $(\beta/\alpha) \times (6.2c)$ to (6.3*b*), we find that (6.3) are also the same equations as (2.19) and (2.20), but this time $(\tilde{u}, \tilde{v}, \tilde{w})$ are replaced by $(u_1 + (\beta/\alpha) w_0, v_1, w_1)$, and $(\mathrm{i}\alpha\tilde{p}_0, \tilde{q}_{0z}, \tilde{A}_0)$ are replaced by

$$\left(\mathrm{i}\alpha p_0 + \frac{\beta}{\alpha}(p_{1z} + \mathrm{i}\beta p_0), \mathrm{i}\beta p_1 + p_{2z}, \tilde{A}_0 \right).$$

In the case $\beta = 0$, equations (6.3) reduce to those for the two-dimensional disturbance, while (6.2) have the trivial zero solution.

Thus the leading-order boundary-layer flow is driven solely by a cross-stream pressure gradient $(p_{1z} + \mathrm{i}\beta p_0)$ which arises because the oblique Tollmien–Schlichting wave has a pressure component perpendicular to the direction of the undisturbed flow. The dispersion relation is determined from the second-order equations in a manner similar to before, but using a skewed velocity and pressure gradient, $(u_1 + (\beta/\alpha) w_0)$ and $(\mathrm{i}\alpha p_0 + (\beta/\alpha)(p_{1z} + \mathrm{i}\beta p_0))$ to take into account the leading-order flow. Hence, for the case $\beta \neq 0$, we obtain the following equation instead of (2.25):

$$(p_{2z} + \mathrm{i}\beta p_1)_z + \psi_0 (p_{2z} + \mathrm{i}\beta p_1) = (\alpha^2 + \beta^2) p_0 - \mathrm{i}\beta p_{1z} + \lambda_0 (\mathrm{i}\alpha^2) A_0 \frac{\mathrm{Ai}'(\xi_0)}{(\mathrm{i}\alpha\lambda_0)^{\frac{1}{3}} K(\xi_1)}. \tag{6.5}$$

Substituting for p_{1z} from (6.4), using the definition of A_0, (2.18), the condition for periodic solutions of (6.5) becomes

$$0 = \left(\alpha^2 I_0 + \frac{\beta^2}{J_0} \right) \hat{p}_0 + \tfrac{1}{2}(\hat{p}_1 - \hat{p}_0) H_0, \tag{6.6}$$

where I_0, J_0 and H_0 are the integrals

$$\left.\begin{aligned} I_0 &= \frac{1}{2\pi/k} \int_0^{2\pi/k} \exp\left[\int_0^z \psi_0 \, \mathrm{d}z \right] \mathrm{d}z,\\ J_0 &= \frac{1}{2\pi/k} \int_0^{2\pi/k} \exp\left[-\int_0^z \psi_0 \, \mathrm{d}z \right] \mathrm{d}z,\\ H_0 &= \frac{1}{2\pi/k} \int_0^{2\pi/k} \exp\left[\int_0^z \psi_0 \, \mathrm{d}z \right] \phi_{yyy}|_{y=0} \frac{\mathrm{Ai}'(\xi_0)}{(\mathrm{i}\alpha\lambda_0)^{\frac{1}{3}} K(\xi_0)} \mathrm{d}z. \end{aligned}\right\} \tag{6.7}$$

As in §2, we can obtain a similar expression to (6.6) from the boundary layer in the upper wall $y = 1$. Eliminating $\hat{p}_0$ and $\hat{p}_1$ between these two equations and simplifying leads to the dispersion relation

$$1 = \frac{1}{2}\left\{\frac{H_0}{\alpha^2 I_0 + \beta^2/J_0} + \frac{H_1}{\alpha^2 I_1 + \beta^2/J_1}\right\}, \tag{6.8}$$

where the integrals I_1, J_1 and H_1 are defined in a similar manner to (6.7) but involving the variables ξ_1, λ_1, etc., corresponding to the upper boundary layer.

It can be seen that in the case $\beta = 0$ (6.8) becomes the dispersion relation for two-dimensional disturbances (2.28). In the case of a two-dimensional flow with no vortex motion, we obtain $I_0 = I_1 = J_0 = J_1 = 1$ and $H_0 = H_1 = \mathrm{Ai}'(\xi)/(\mathrm{i}\alpha\lambda)^{\frac{1}{3}}K(\xi)$, so that (6.8) would reduce to

$$(\alpha^2 + \beta^2) = \frac{\mathrm{Ai}'(\xi)}{(\mathrm{i}\alpha\lambda)^{\frac{1}{3}}K(\xi)}$$

which is, of course, the usual eigenrelation for three-dimensional disturbances. We can also find the asymptote of (6.8) as $\Omega \to \infty$ in a manner similar to that outlined in §4. If

$$\gamma = \frac{\beta}{\alpha}$$

is real then (4.9) still holds:

$$\alpha \sim C_1 \Omega^{\frac{1}{3}} - \mathrm{e}^{\mathrm{i}\pi/4} C_2 \Omega^{-\frac{5}{6}} \quad \text{as } \Omega \to \infty,$$

but now the constants C_1 and C_2 are defined by

$$C_1^3 = \frac{1}{2}\sum_{j=0}^{1} \frac{\Phi_j}{L_{j,-1} + \dfrac{\left(\dfrac{2\pi\gamma}{k}\right)^2}{L_{j,1}}},$$

$$C_2 = \frac{1}{6C_1}\sum_{j=0}^{1} \frac{\Phi_j\left(\dfrac{2\pi}{k} + \left(\dfrac{2\pi\gamma}{k}\right)^2 \dfrac{L_{j,2}}{(L_{j,1})^2}\right)}{\left(L_{j,-1} + \dfrac{\left(\dfrac{2\pi\gamma}{k}\right)^2}{L_{j,1}}\right)^2},$$

where Φ_0 and Φ_1 are given in §4 and

$$L_{j,n} = \int_0^{2\pi/k} \lambda_j^n \, \mathrm{d}z, \quad j = 0, \quad n = -1, 1, 2.$$

We postpone a discussion of the numerical results we have obtained for this eigenrelation until the next section.

7. Results and discussion

We shall concentrate our attention on the effect of longitudinal vortices on the growth rate of Tollmien–Schlichting waves. Though there is some interest in the effect of the vortices on the neutral curve for the Tollmien–Schlichting wave, it is the effect of the vortices on the growth rates which will be most relevant to the closely related external-boundary-layer problem. In any case our calculations indicate that large-amplitude vortices have little effect on the neutral configuration whilst even

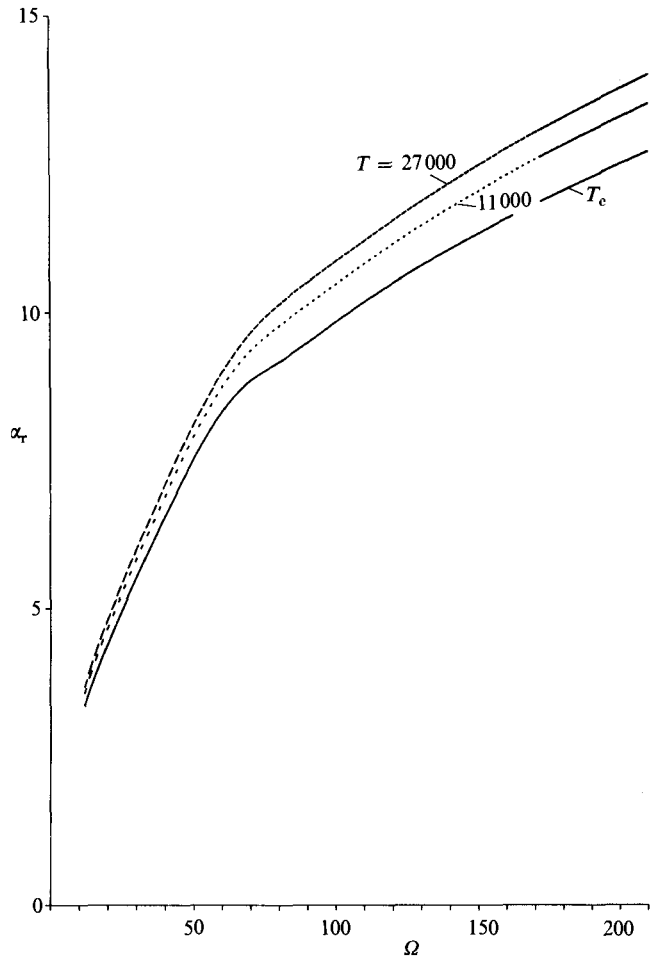

FIGURE 7. The wavenumber α_r as a function of Ω for several values of T with $\beta = 0$.

small-amplitude vortices significantly alter the growth rates in the unstable regime.

In figures 7 and 8, we show the wavenumber and growth rate of two-dimensional Tollmien–Schlichting waves at different values of the Taylor number T. The results shown correspond to $k = k_c = 3.951$ the critical wavenumber of linear theory for Taylor–Görtler vortices. The vortices have little effect on the neutral frequency and the size of the largest amplification rate. We see in figure 8 that at most frequencies the amplification rate increases monotonically with T. For $T > 27000$ the Taylor vortex could not be calculated because it was apparently unstable to a vortex with twice the spanwise wavenumber of the most dangerous mode of linear theory. The frequency corresponding to the maximum growth rate increases with T. Moreover, the growth rates beyond the maximum are significantly increased for Ω less than about 100. This result is of particular importance to the control of external boundary layers if a similar result holds for such flows. Certainly the known similarities between the lower-branch structures for Poiseuille flow and Blasius flow make that likely, but there are difficulties in applying the theory to external flows. The major difficulty is surprisingly not the effect of boundary-layer growth, which can be taken care of as in Smith (1979*b*), but the lack of a nonlinear theory for Görtler vortices in

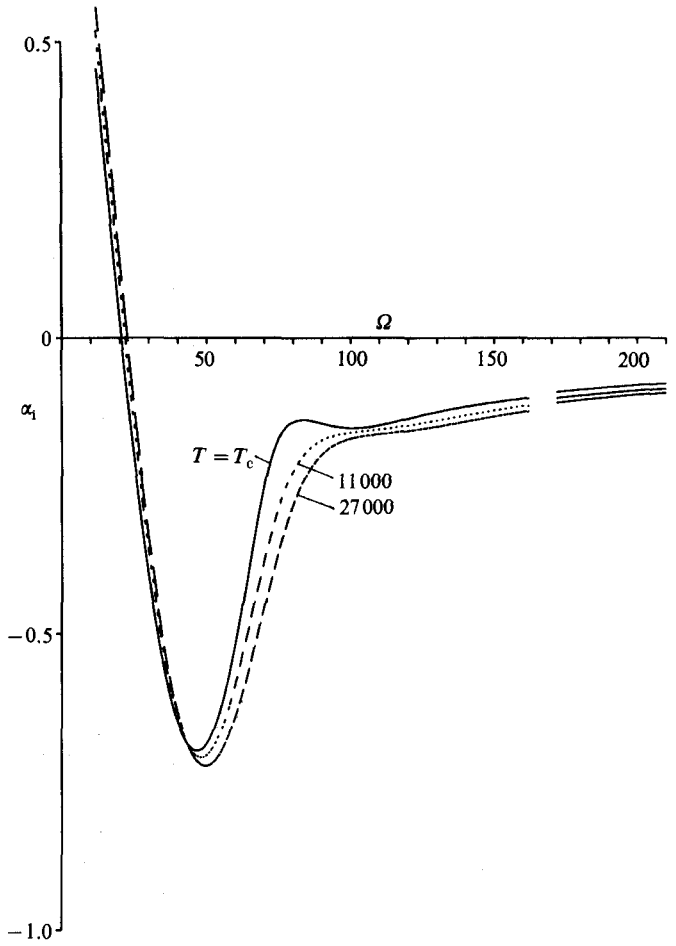

FIGURE 8. The growth rate α_i as a function of Ω for several values of T with $\beta = 0$.

growing boundary layers. Thus, though our approach of §3 is readily applied to external flows, the absence of any knowledge of even weakly nonlinear Görtler vortices at $O(1)$ wavenumbers prevents us from completing such an investigation.

For external flows, the local Tollmien–Schlichting frequency increases as the wave travels downstream and the growth rate adjusts locally. Thus the total growth of the disturbance can be found by integrating the growth rate in the streamwise direction. In this context the increased growth rates shown in figure 8 to the right of the maximum are possibly significant. As a measure of the destabilization produced by the vortices, we can calculate the area between the different curves and the $\alpha_i = 0$ axis for $20 < \Omega < 100$. Such a calculation shows that for $T > 11000$ the area is about 10% greater than that for Poiseuille flow. Thus for external flows which can support Görtler vortices it is possible that their presence might cause the premature growth of Tollmien–Schlichting waves. The effect of finite-amplitude vortices on the Tollmien–Schlichting wavenumber is shown in figure 7. The wavenumber increases monotonically with T, but the rate of increase is very small between $T = 19000$ and 27000.

In figures 9 and 10 we compare the results for the weakly nonlinear theory when $A = 0.145$ with the fully nonlinear vortex calculations at the corresponding Taylor

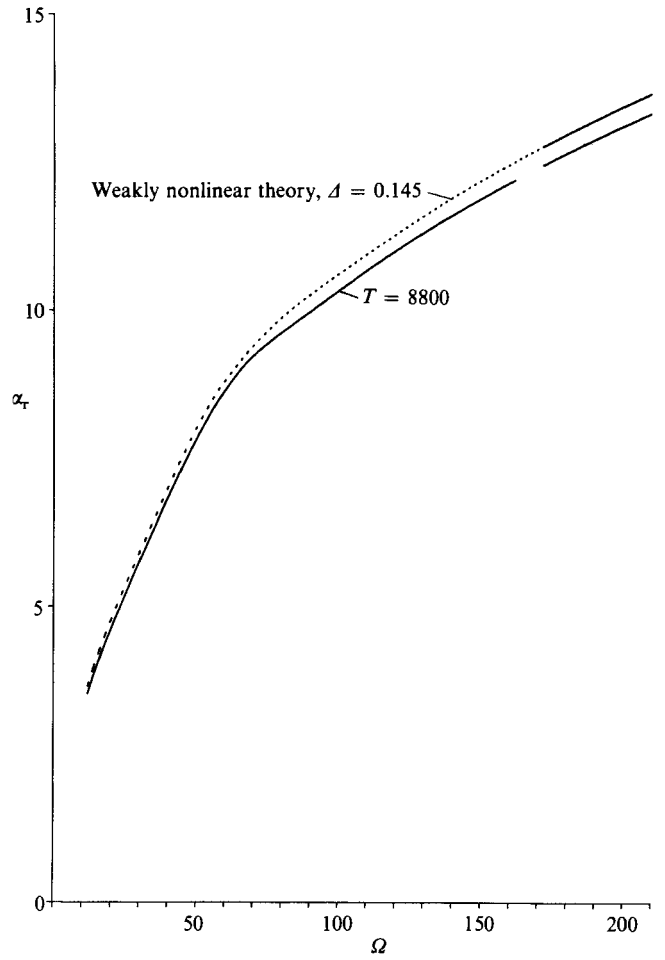

FIGURE 9. The wavenumber α_r as a function of Ω for $T = 8800$ compared with the corresponding weakly nonlinear prediction.

number $T = 8800$. These figures show reasonable agreement for all values of Ω. Figure 11 shows how the critical frequency of the Tollmien–Schlichting waves, Ω_c, varies as the Taylor number is increased from T_c to its maximum value of 27 000. Also shown is the behaviour predicted by the weakly nonlinear theory, which is accurate for T up to about 7000, $A = 0.1$.

The dispersion relation for oblique Tollmien–Schlichting waves is shown in figures 12 and 13 for $T = 11000$ and for $\beta/\alpha = 0$, $1/\sqrt{3}$, 1, $\sqrt{3}$, corresponding to waves travelling parallel, at 30°, 45° and 60° to the direction of the flow. The results are qualitatively the same as the situation when there are no vortices present: the waves travelling parallel to the flow having maximum growth rate.

We should note that for the channel problem Tollmien–Schlichting instabilities might be expected to occur first at finite Reynolds numbers. For external flows this is also possible, but there it seems more natural to make a high-Reynolds-number approximation since there would not be a boundary layer unless the Reynolds number were large. Thus it might be argued for external flows that the most significant linear instability calculation is one that calculates the amplification rates between the upper and lower branches of the neutral curve. Since the motivation for

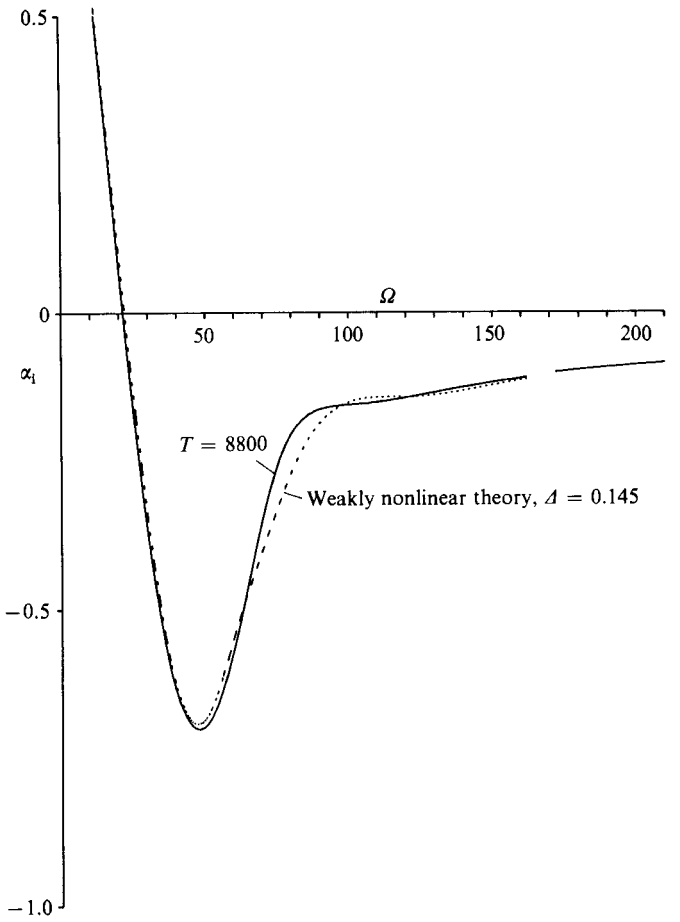

FIGURE 10. The growth rate α_i as a function of Ω for $T = 8800$ compared with the corresponding weakly nonlinear prediction.

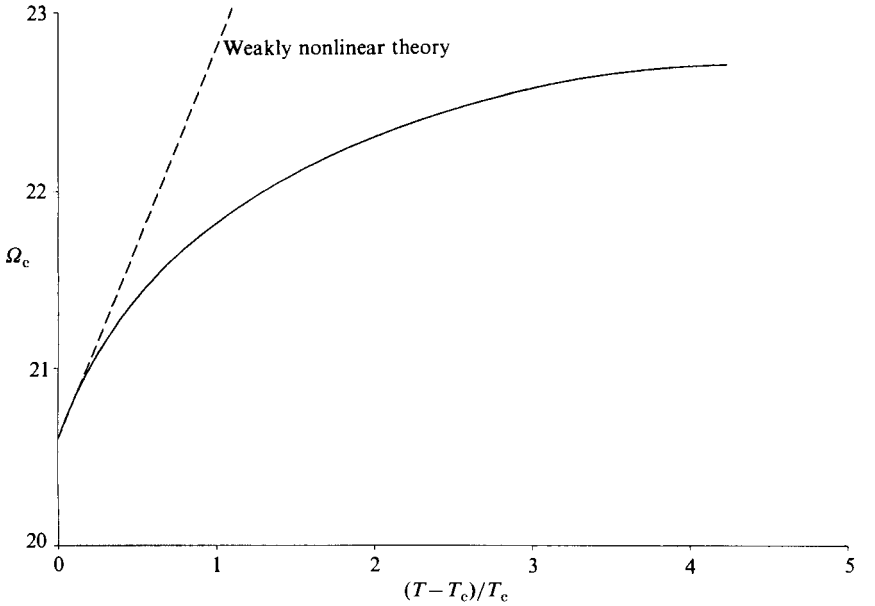

FIGURE 11. The critical frequency of the Tollmien–Schlichting waves Ω_c plotted against the Taylor number.

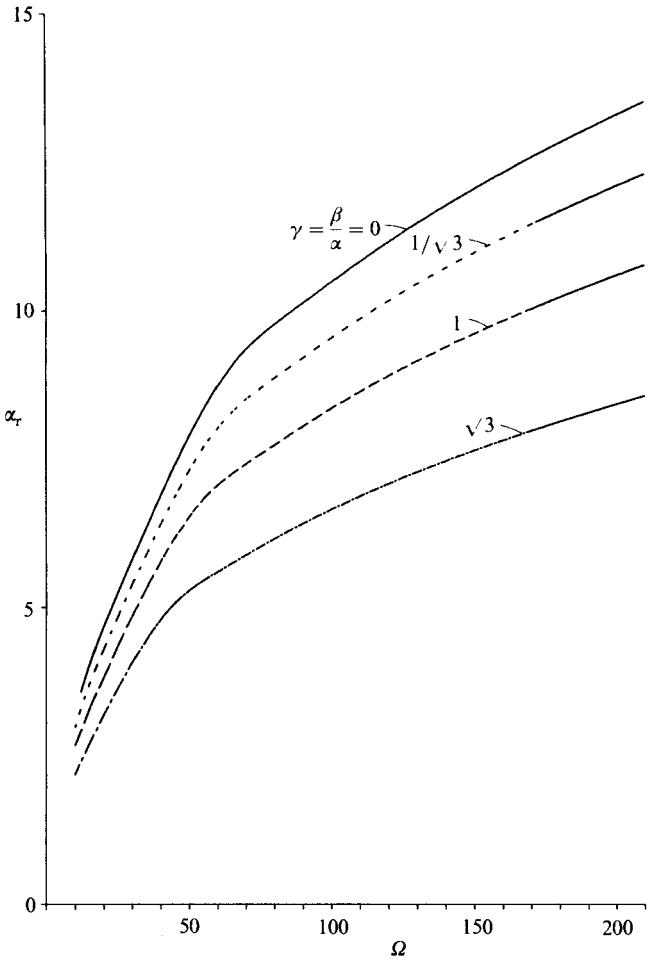

FIGURE 12. The wavenumber α_r as a function of Ω for $T = 11000$ with $\beta/\alpha = 0$, $1/\sqrt{3}$, 1, $\sqrt{3}$.

our calculation was to shed light on the possible effects of longitudinal vortices on Tollmien–Schlichting waves in boundary layers, we feel that a large-Reynolds-number assumption is sensible. We note however that at finite Reynolds numbers the normal and spanwise velocity components of the longitudinal vortex are no longer negligible and the z-dependence of the vortex does not become parametric in any region of the flow. Thus at finite Reynolds number the computations required would be significantly larger than those discussed here.

Our aim in this work has been to find the effect of finite-amplitude longitudinal vortex structures on the growth of infinitesimal Tollmien–Schlichting waves in curved channel flows. We have ignored the possibility that the vortices become unstable to time-dependent non-axisymmetric vortex modes of the type that lead to the onset of wavy vortex flows in the Taylor problem. We note that Hall (1982*b*) has shown that such disturbances occur in external flows over curved walls so this possible mechanism for the onset of a time-periodic secondary instability should not be ignored. However, if the latter mode does indeed occur in curved channel flows, the question of whether it or Tollmien–Schlichting waves are the cause of the secondary instability of Taylor–Görtler vortices can only be answered by a nonlinear analysis.

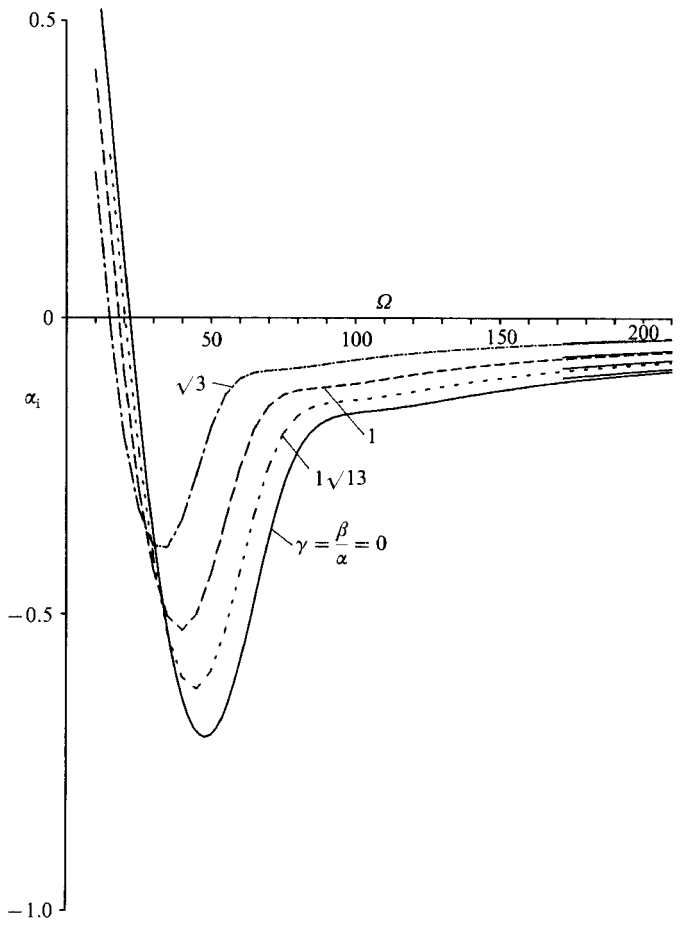

FIGURE 13. The growth rate α_i as a function of Ω for $T = 11000$ with $\beta/\alpha = 0$, $1/\sqrt{3}$, 1, $\sqrt{3}$.

The first author was supported by the SERC while this work was completed. Research for the second author was supported under NASA Contract No. NAS1-18107 while in residence at the Institute for Computer Applications in Science and Engineering (ICASE), NASA Langley Research Center, Hampton, VA 23665.

REFERENCES

ABRAMOWITZ, M. & STEGUN, I. A. 1965 *A Handbook of Mathematical Functions*. Dover.

BENNETT, J. 1986 Theoretical properties of three dimensional interactive boundary layers. Ph.D. thesis, University of London.

DEAN, W. R. 1928 Fluid motion in a curved channel. *Phil. Mag.* **5**, 673.

FASEL, H. & BOOZ, I. 1984 Numerical investigation of supercritical Taylor vortices in the wide gap limit. *J. Fluid Mech.* **138**, 21–52.

HALL, P. 1982*a* Taylor–Görtler vortices in fully developed or boundary-layer flows: linear theory. *J. Fluid Mech.* **124**, 475–490.

HALL, P. 1982*b* On the non-linear evolution of Görtler vortices in non-parallel boundary layers. *IMA J. Appl. Maths* **29**, 173–196.

HALL, P. 1983 The linear development of Görtler vortices in growing boundary layers. *J. Fluid Mech.* **130**, 41–59.

HALL, P. & BENNETT, J. 1986 Taylor–Görtler instabilities of Tollmien–Schlichting waves and other flows governed by the interactive boundary-layer equations. *J. Fluid Mech.* **171**, 441–457.

NAYFEH, A. H. 1981 Effect of streamwise vortices on Tollmien–Schlichting waves. *J. Fluid Mech.* **107**, 441–453.

ROGERS, E. H. & BEARD, D. W. 1969 A numerical study of wide-gap Taylor vortices. *J. Comp. Phys.* **4**, 1.

SEMINARA, G. 1976 Instability of some unsteady viscous flows. Ph.D. thesis, University of London.

SMITH, F. T. 1979*a* Instability of flow through pipes of general cross-section. *Mathematika* **26**, 187–210.

SMITH, F. T. 1979*b* On the non-parallel flow stability of the Blasius boundary layer. *Proc. R. Soc. Lond.* A **368**, 573.